ACADEMIA ROMÂNĂ
Revue Roumaine de Chimie
http://web.icf.ro/rrch/

Rev. Roum. Chim.,
2021, *66*(6), 479–491
DOI: 10.33224/rrch.2021.66.6.01

KINETIC MODELS OF AQUEOUS 2-MERCAPTOBENZOTHIAZOLE ADSORPTION ON LOCAL CLAY AND ACTIVATED CARBON

Nouzha BOUZIANE,[a] Amel ALOUI,[a] Samia BEHLOUL[a,b] and Abdennour ZERTAL[a,*]

[a]Innovative Techniques of Environment Preservation Laboratory, Mentouri Brothers University – Constantine 1. Aïn El-Bey Street, 25000 Constantine, Algeria
[b]Department of Chemistry, Faculty of Material Sciences, Hadj Lakhdar University Batna 1, 05000 Batna, Algeria

Received January 13, 2020

Adsorption of 2-mercaptobenzothiazole (MBT) onto local bentonite (BN) and activated carbon (AC) in aqueous solution was investigated in batch system. The experimental kinetic data were given by the residual concentration fraction of solute versus contact time. For both adsorbents, the adsorption process was instant in the early stage. This behaviour prompted us to develop the new two and three-stage kinetic models. The adsorption kinetics of MBT onto AC and BN matches well with the two-stage and the three-stage kinetic models, respectively. Experimental data were also correlated with many other kinetic models as well as the pseudo-second order. Retention rate appears to be mainly controlled by intraparticle diffusion. The process follows multiple sorption rates with AC. This was essentially attributed to the presence of different pore sizes in its structure. It was shown that the two proposed kinetic models could best describe the adsorption kinetics of MBT onto AC and BN.

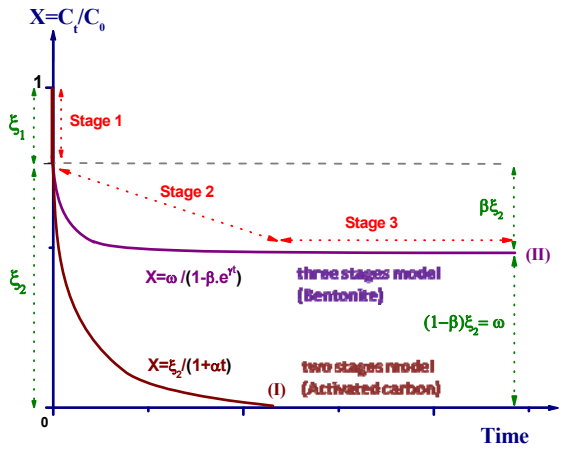

INTRODUCTION

In recent years an increasing attention has been paid to the elimination of toxic and recalcitrant organic pollutants present in industrial wastewaters and in landfill leachates. Among various disposal treatment methods, adsorption is considered to be one of the best-known, the most studied and applied separation techniques, particularly in industrial-scale.[1,2] In this context, and over the past three decades, a considerable number of studies had aimed to clarify the phenomenon of retention, to control the treatment process and to ensure its effectiveness. Thus, several mathematical models were developed and applied to the experimental results in order to control the kinetics and to give a clearer understanding of the sorption mechanism. Nowadays, it is almost certain of the existence of several kinetic stages during the adsorption of a solute. However, the retention evolution of the molecule is often described by three steps: a first step very fast (instant step) where the adsorbate is transported from the bulk phase to the exterior surface of the adsorbent. Followed by a slow step regarding the diffusion of molecules to internal sites, it is the rate-limiting step, and then a step where the adsorption process remains constant (equilibrium).[3-6] On the other hand, developers and usually applied empirical kinetic expressions such as the pseudo-first and pseudo-second-order

* Corresponding author: azertal@hotmail.com

equations and Elovich model do not allow the distinction between these three phases.

In aqueous solution, a new model, based on the solute mass conservation, was proposed.[7-11] This model has the advantage to take into account the different phases of the adsorption process. However, this model describes the kinetics of two and three stages with the same equation developed on the basis of the intraparticle release.[8] That is why there was a significant difference between the curves generated by the kinetic model of two stages and practical values in the adsorption of many products. In fact, it was not possible to limit the final step in these cases.

Among the most used adsorbents in the research, and also in the industry, the activated carbons from different resources as well as the raw or activated mineral clays have been the subject of numerous studies. If the activated carbon is considered as the most important adsorbent due to its many properties such as large surface area, microporous structure and cost effectiveness, mineral clays have the advantage to be available with a lower price and play an important role in the production of drugs and in the wastewaters treatment.

2-Mercaptobenzothiazole (MBT), selected as a model pollutant, is a toxic xenobiotic and poorly biodegradable in environment. It is generally used in the production of rubber additive chemicals but is predominately as vulcanization accelerator in rubber industry.[12] It also has other uses and has been extensively detected in wastewater effluents and sewage treatment plant, especially in surface water, where it persists for several weeks.[13]

In this study, alternative models based on the three stages model, proposed in the literature in order to account for the rapid and slow adsorption, were developed. Significant changes have been done to simplify the proposed equations. Application of the new models for the removal of MBT by AC and BN from aqueous solutions in batch system is presented. Fundamental kinetic data and new information on the mechanism of adsorption using many simplified kinetic models, Weber and Morris, Boyd, Urano and Tachikawa, Elovich, Avrami and pseudo-second order, are obtained and compared. All equations are described by the residual concentration fraction of solute versus contact time.

THEORETICAL

Evolution of the residual concentration fraction of a solute *versus* contact time can be described by one of the two possible curves shown in Figure 1. Each curve reflects the presence of two or three stages during adsorption process. The first stage is very fast and instant, then the second and/or the third different from one case to another.

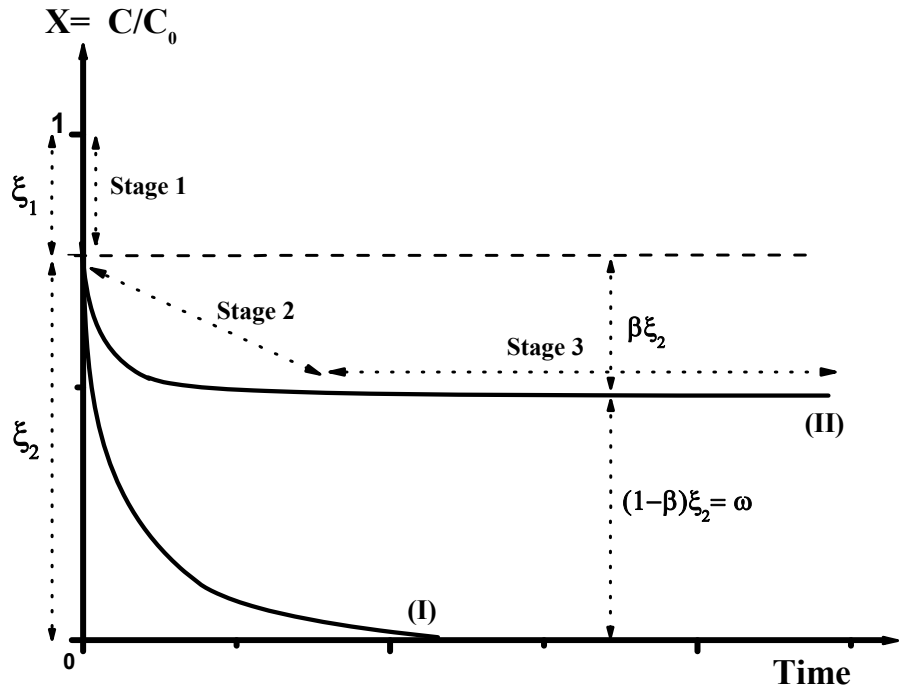

Fig. 1 – Evolution of the residual concentration fraction of a solute *vs* adsorption time (two and three stages models).

In the case of two stages model (curve I), the first phase is described by the parameter $\xi_1 = \frac{C_1(\infty)}{C_0} = \frac{Mq_1(\infty)}{VC_0}$, defined as the solute fraction used during this stage. C_0 and $C_1(\infty)$ are the initial and final solute concentration respectively, M the adsorbent mass, $q_1(\infty)$ the adsorbed solute amount per unit mass of sorbent and V the solution volume.[8] The second phase, corresponding to the mass transfer from the aqueous phase to the inland sites, is less rapid and can be characterized by the parameter $\xi_2 = \frac{C_2(\infty)}{C_0} = \frac{Mq_2(\infty)}{VC_0}$, fraction of the adsorbed solute. $C_2(\infty)$ is the solute final concentration, $q_2(\infty)$ the adsorbed solute amount per unit mass of sorbent at infinity and $\xi_1 + \xi_2 = 1$.

The adsorption rate is given at any time by the following equation:[7,8]

$$\frac{\partial C(t)}{\partial t} = -\alpha . C(t)\left[1 - \frac{q_2(t)}{q_2(\infty)}\right] \quad \text{(Eq.1)}$$

where C(t) and $q_2(t)$ are, respectively, the solute concentration and the adsorbed solute amount per unit mass of sorbent at time t and α the rate constant characterizing the second phase of adsorption.

Nevertheless, the solute mass balance equation is given by:

$$V.C(t) + M.[q_1(t) + q_2(t)] = V.C_0 \quad \text{(Eq.2)}$$

where $q_1(t) = q_1(\infty)$.

Taking into account the expressions of ξ_1 and ξ_2 yields:

$$X - \frac{C(t)}{C_0} - \xi_2\left[1 - \frac{q_2}{q_2(\infty)}\right] \quad \text{(Eq.3)}$$

However, it is easy to make appear the *X* term in Eq.(1) :

$$\frac{\partial(X)}{\partial t} = -\alpha X\left[1 - \frac{q_2}{q_2(\infty)}\right] \quad \text{(Eq.4)}$$

Then, the two Eqs.(3) and (4) gives :

$$\frac{\partial X}{X^2} = -\frac{\alpha}{\xi_2}\partial t \quad \text{(Eq.5)}$$

Taking into account the boundary conditions, *t* = 0 to *t* and *X* = ξ_2 to *X*, the integration of Eq. 5 leads to:

$$\frac{1}{X} = \frac{1}{\xi_2} + \frac{\alpha}{\xi_2}t \quad \text{(Eq.6)}$$

This is the linear form of the following equation:

$$X = \frac{\xi_2}{1 + \alpha t} \quad \text{(Eq.7)}$$

A new kinetic parameter can be defined from the Eq.(4), it is the reduced adsorption rate: $r^* = -\frac{\partial(X)}{\partial t}$, which can be written as :

$$r^* = \frac{\alpha.\xi_2}{(1 + \alpha t)^2} = \frac{\alpha}{\xi_2}.X^2 \quad \text{(Eq.8)}$$

at *t* = 0, X = ξ_2 and $r_0^* = \alpha.\xi_2$.

In the case of three-stage model (curve II), the first phase is similar to that of the curve I, *i.e.* fast and instant. It is therefore described by a similar parameter ξ_1.

On the other hand, the curve allure of the second phase, corresponding to the mass transfer, is different. Therefore, it is necessary to introduce the limiting factor β in Eq.1 and β must be less than 1. The adsorption rate expression wills be:[7,8]

$$\frac{\partial C}{\partial t} = -\alpha C\left[1 - \frac{q_2(t)}{\beta q_2(\infty)}\right]$$

$$\frac{\partial X}{\partial t} = -\alpha X\left[1 - \frac{q_2(t)}{\beta q_2(\infty)}\right] \quad \text{(Eq.9)}$$

according to Eq.3:

$$\frac{q_2(t)}{q_2(\infty)} = 1 - \frac{1}{\xi_2}X$$

We have

$$\frac{\partial X}{\partial t} - \frac{\alpha}{\beta\xi_2}X[(1-\beta)\xi_2 - X] \quad \text{(Eq.10)}$$

Separating the variables in this equation gives:

$$\frac{\partial X}{X(X-\omega)} = -\frac{\alpha}{\beta\xi_2}\partial t \quad \text{(Eq.11)}$$

with $\omega = (1-\beta).\xi_2$

Integrating this for the boundary conditions gives:

$$\int_{\xi_2}^{X}\frac{\partial X}{X(X-\omega)} = -\frac{\alpha}{\beta\xi_2}\int_0^t \partial t$$

$$\ln\frac{1}{\beta}\left(1 - \frac{\omega}{X}\right) = -\frac{\alpha\omega}{\beta\xi_2}t = -\frac{\alpha}{\beta}(1-\beta)\,t \quad \text{(Eq.12)}$$

X may be calculated as follows:

$$X = \frac{(1-\beta)\,\xi_2}{1-\beta\, e^{-\gamma t}} = \frac{\omega}{1-\beta\, e^{-\gamma t}} \quad \text{(Eq.13)}$$

with $\gamma = \frac{\alpha}{\beta}(1-\beta)$

On the other hand, the reduced adsorption rate can also be expressed depending on time or according to the fraction *X*:

$$r^* = -\frac{\partial(X)}{\partial t} = \frac{\alpha.\xi_2.(1-\beta)^2.e^{-\gamma t}}{(1-\beta e^{-\gamma t})^2} = \gamma.X\left(\frac{X}{\omega} - 1\right) \quad \text{(Eq.14)}$$

at $t = 0$, $X = \xi_2$ and $r_0^* = \alpha.\xi_2$.

The third phase of this model is characterized by a constant residual. We can therefore write $X = (1-\beta) \times \xi_2 = \omega$. At this stage, equilibrium, the adsorption rate is equal to the desorption rate. It should be noted finally that the solute removal efficiency can also be expressed versus *X*. Actually, $R_t = (C_0\text{-}C_t)\text{–}100/C_0$, thus $R_t = (1\text{–}X)\times 100$. Indeed, The final performance $R_{t\infty}$ is 100% and $(1-\omega)\times 100\%$ for activated carbon and bentonite, respectively.

RESULTS AND DISCUSSION

Textural properties of Adsorbents

The microtextural properties of AC and BN used in this study are presented in Table 1. According to the data of this table, AC seems to have a specific surface area twice and a half larger than that of BN. This parameter is important in the discussion of the two adsorbents effectiveness. Moreover, the pore size distribution shows that both adsorbents present a broad pore structure. The most pore volume (81%) of AC has diameters between 6 and 80 nm, while BN include more than 40% of pore volume with diameters over 80 nm.

Adsorption kinetics

The evolution of the MBT concentration as function of contact time with AC and BN is shown in Figure 2. The allure of the adsorption kinetics reveals various behaviours and therefore different adsorbent-adsorbate affinity.

Experimental results of MBT adsorption on AC in aqueous solution are shown on Figure 2a, which clearly shows the almost total disappearance of the substrate after 20 minutes of contact, more than 99.99%, which demonstrates the high efficiency of this adsorbent. This figure also shows that the fraction *X vs* time can be divided into two distinct stages: the first stage, instant and very fast, corresponds to a significant elimination of MBT, about 30%, while the second stage, which is slower, leads to its total elimination. From a Modelling point view, the experimental points allure orient directly towards the two stage model. Indeed, application of Eq. 8, curve of Figure 2a, shows the correlation was almost perfect between the experimental and theoretical results as also shown by the straight line described by Eq. 7 (Figure 2a insert). The resulting straight line has been used to calculate both ξ_2 and α parameters and then the value of ξ_1 was deduced. The obtained values are given in Table 2.

In the case of bentonite, the adsorption process evolves into three phases: a first phase very fast and very short followed by a quick adsorption then the saturation phase. Thus, the equilibrium plateau is quickly reached. 5 minutes only have been enough to reach the maximum rate of adsorption which is approximately 46%. Therefore, the substrate elimination is not total and less than 5% of MBT are retained in the first stage (Fig. 2b). The experimental points are presented at the same time as the theoretical curve described by Eq.14. Figure 2b clearly shows the good correlation between theoretical and experimental data as also confirmed by the high value of the correlation coefficient, more than 0.994, characterizing the straight line corresponding to Eq.12. The X_∞ value, which is other than the constant ω, is 0.54. It allows deducing the final adsorbed amount, which is 9.2 $mg.g^{-1}$. It is slightly less than half of the MBT initial amount.

As it can be seen in Figure 2, activated carbon is more effective than Bentonite for the MBT elimination from aqueous solution. This was somewhat expected given the very significant difference between the specific surfaces of the two adsorbents.

Furthermore, results of r* calculation are summarized in Table 3. During the first stage, decrease of r* is faster with AC than that obtained with BN. This can be attributed to the number of available adsorption sites and therefore to the specific surface of each adsorbent. Thus, in the case of AC, the value of r* decreases from 2,133 to 1,499 min^{-1}, 30% of reduction, then becomes almost zero after 10 minutes of contact, while there is a decrease of r* from 1.092 to 1.044 min^{-1} with BN, which means only 4% of reduction. Thus, the first phase is characterized by a very low value of ξ_1. Subsequently, r* passes to lower values during the second phase of adsorption and vanish almost after 5 min of contact. In this case, the third phase

is characterized by adsorption rate virtually zero (attainment of equilibrium). All results of r* calculations are in good agreement with those of Figure 2 for both adsorbents.

Table 1

Surface area and pore size distribution of adsorbents

Adsorbents		**AC**	**BN**
BET Surface area (m^2/g)		99.770	40.434
Average Particle Size (µm)		80 <**d**< 100	1<**d**< 2
		Pore Volume (mL/g)	
Pore Diameter Range (nm)	< 6	0.02685 *(12.99%)*	0.00787 *(4.56%)*
	6 < PDR < 20	0.09164 *(44.35%)*	0.02912 *(16.90%)*
	20 < PDR < 80	0.07562 *(36.59%)*	0.06479 *(37.58%)*
	Over 80	0.01255 *(6.07%)*	0.07062 *(40.96%)*

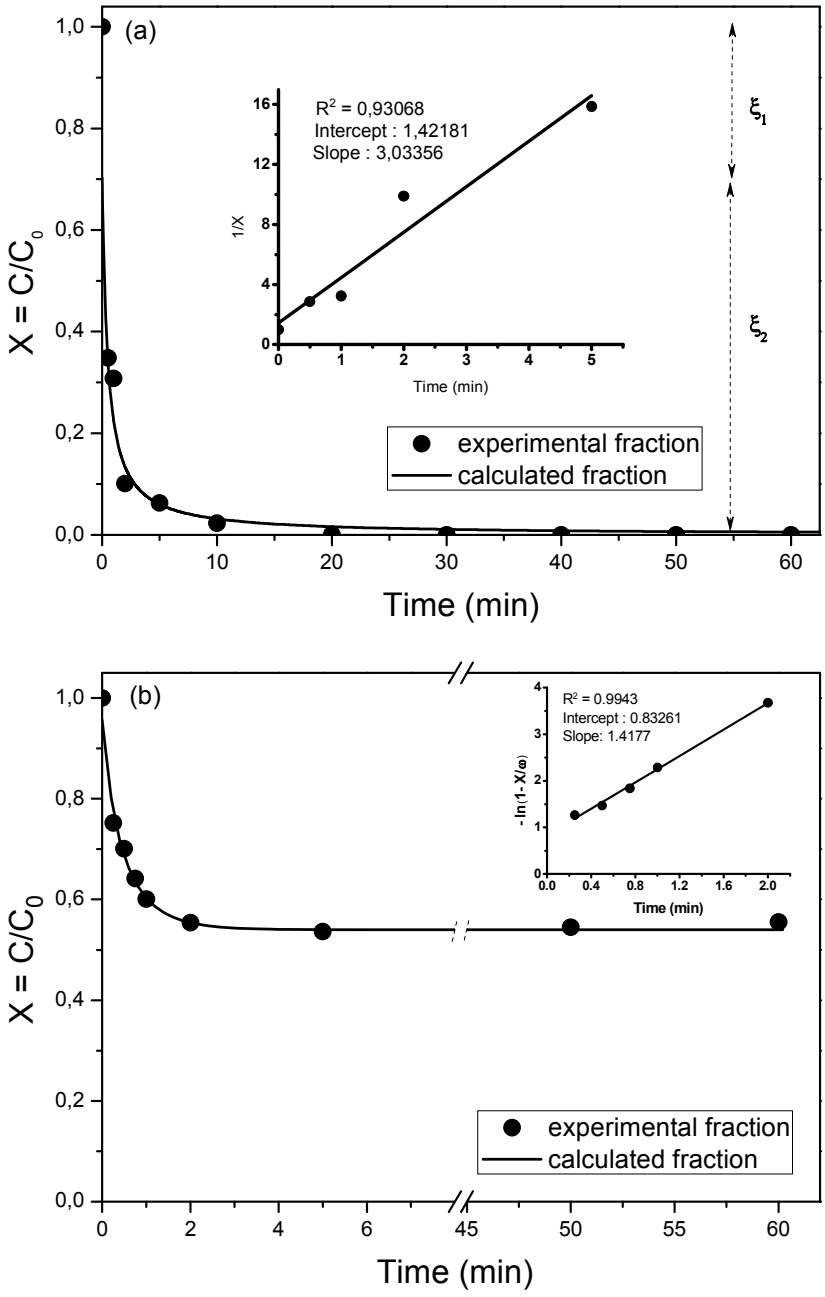

Fig. 2 – Evolution of the residual concentration fraction of MBT
(C_0 = 20 mg.L^{-1}, m_{ads} = 0.5 g.L^{-1}, pH ≈ 6.5 et T = 20 ±1 ^{0}C)*vs* adsorption time : (a) AC, (b) BN.

Table 2

Values of two and three stage kinetic model parameters

	ξ_1	ξ_2	ω	γ	α (min^{-1})	β	R_∞ (%)
AC	0.297	0.703	/	/	2.133	/	100
BN	0.044	0.956	0.540	1.418	1.092	0.435	46

Table 3

Evolution of the reduced adsorption rate (r^*) *vs* contact time

Time (min)	**AC**	**BN**
	First stage	
0	2.133	1.092
	Second stage	
0	1,499	1.044
0,5	0,367	0,276
1	0,288	0,100
2	0,031	0,021
5	0,012	$2{,}73\times10^{-4}$
10	0,002	$2{,}28\times10^{-7}$

Kinetic models

Weber and Morris Model

Among the models that allow to have information on the stages of the adsorption process, the intraparticle diffusion model was widely used to describe and understand the transport of solute from the external surface to the pores of the adsorbent.[14,15] It is well described by Weber and Morris equation:

$$q_t = k_i.t^{1/2} + b \qquad \text{(Eq.15)}$$

with, k_i : intraparticle diffusion rate constant, b: constant.

The Weber and Morris equation becomes:

$$1 - X' = k_i'.t^{0.5} + b' \qquad \text{(Eq.16)}$$

where $k_i' = ki/q_2(\infty)$, b' = $b/q_2(\infty)$ and X' = X/ξ_2. Intraparticle diffusion is seen as limiting step of the adsorption process if the straight line (1-X') = f ($t^{1/2}$) passes through the origin (*i.e.*, b' = 0). The parameters k_i' and b' can be obtained from the straight line plots of (1-X') versus time and then the values of *ki* and *b* are deduced. All straight lines obtained in Figure 3 present good regression coefficients (R^2), their values are ranged between 0.9911 and 0.9992. In the case of activated carbon adsorption, in two stages, Figure 3 shows the presence of two straight lines in addition to one that matches the saturation. Unlike the second, the first straight line passes through the origin. Therefore, intraparticle diffusion may be the only mechanism controlling the adsorption process. In addition, the two lines have very different slopes. Indeed, the slope of the second is less important than that of the first (Table 4). These results allowed deducing the diffusion constants (k_i). The first right is characterized by a k_i of 17.11 $mg.g^{-1}.min^{-1}$ almost ten times more important than that of the second right, which shows a significant change in the rate of diffusion. This can be explained by the decrease of the solute molecules number in the aqueous solution and/or the presence of different sizes of pores (macropores, mesopores and micropores). It is well accepted that the rate of the diffusion constant is closely linked to the size of the pores of the solid; it reduces passing to another smaller pore size.[15,16] One speaks then about the macro and the micro diffusion.[17] Moreover Figure 3 shows a single linear evolution with a very good regression coefficient (0.9977). In addition, the straight line passes very near the origin, implying that the intraparticle diffusion also plays an important role in rate determining step. Unlike the case of active carbon, the local clay seems to present a uniform porosity. In this case, the obtained values of ki' and ki are 0.3804 min^{-1} and 14.55 $mg.g^{-1}\cdot min^{-1}$, respectively (Table 4). The diffusion rate through BN is therefore slightly less rapid than that recorded with AC. This can be attributed to the difference between the specific surfaces of two adsorbent. It should be

noted that, in the case of clay, it's the transfer of MBT molecules across the boundary in solution to the interfoliar space layer constituting the structure of Bentonite.

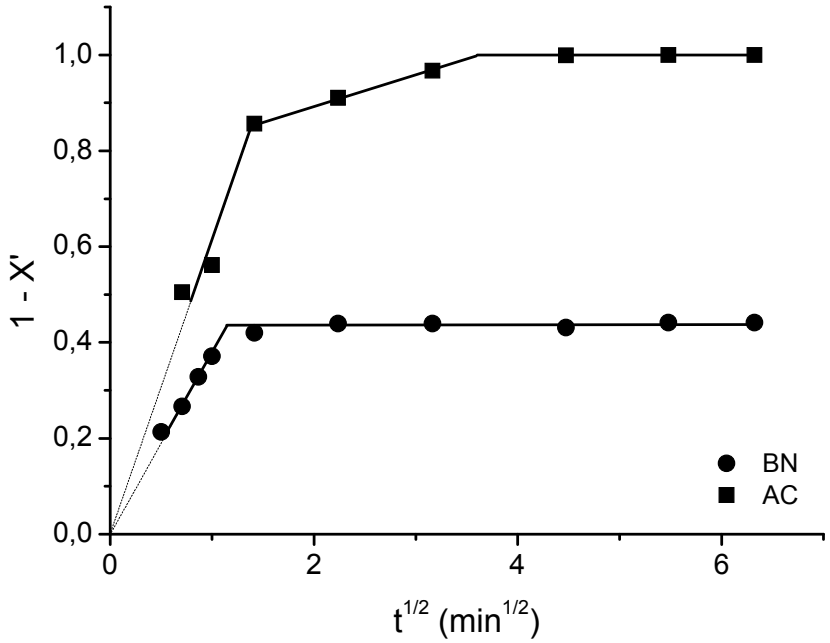

Fig. 3 – Weber and Morris plots for the kinetic modelling of MBT adsorption.

Table 4

Synthesis of the kinetic parameters of MBT adsorption on activated carbon and bentonite using different kinetic models

Weber and Morris

	1st straight line				2nd straight line		
	$q_2(\infty)$ (mg.g^{-1})	k_i' (min$^{-1/2}$)	k_i (mg.g^{-1}.min$^{-1/2}$)	R^2	k_i' (min$^{-1/2}$)	k_i (mg.g^{-1}.min$^{-1/2}$)	R^2
AC	28.12	0.6086	17.11	0.9911	0.0634	1.78	0.9992
BN	38.24	0.3804	14.55	0.9977		/	

Boyd

	1st straight line		2nd straight line	
	B	R^2	B	R^2
AC	0.86619	0.88346	0.18664	0.99215
BN	1.58577	0.99473	/	

Urano and Tachikawa

	1st straight line			2nd straight line		
	k_i	D_i/d^2	R^2	k_i	D_i/d^2	R^2
AC	0.72161	$1.83.10^{-2}$	0.86894	0.17953	4.55	0.99004
BN	1.44315	$3.65.10^{-2}$	0.99332		/	

Elovich

	1st straight line					2nd straight line				
	b'	*b*	*a*	1/(ab)	R^2	*b'*	*b*	*a*	1/(ab)	R^2
AC	3.945	0.1403	89.41	0.08	0.7355	15.676	0.5575	6.05×10^5	$< 10^{-5}$	0.9867
BN	9.540	0.2495	118.72	0.03	0.9710			/		

Avrami

	1st straight line				2nd straight line			
	n	lnk	k	R^2	n	lnk	k	R^2
AC	0.597	0.1786	1.1955	0.9941	0.391	0.6313	1.8800	0.9919
BN	0.800	0.7777	2.1765	0.9757		/		

Boyd Model

In order to ascertain the rate-controlling step, the Boyd (1947) model was also applied to the adsorption kinetic data. This model is generally given by the following equation:[18,19]

$$F = 1 - \frac{6}{\pi^2}\sum_{1}^{\infty}(1/n^2)\exp(-n^2 B.t) \quad \text{(Eq.17)}$$

where $F=q_t/q_e$ is the fractional attainment of equilibrium at time *t*, *n* is a constant and *B* is Boyd constant. This equation can be written and simplified as follows:[20]

$$B.t = -\ln(1 - F) - 0.4977 \quad \text{(Eq.18)}$$

In the case of activated carbon, we can write:

$$B.t = -\ln(X') - 0.4977 \quad \text{(Eq.19)}$$

with bentonite, we must take into account the β coefficient, F will be given by:

$$B.t = -\ln\left[1 - \left(\frac{1 - X'}{\beta}\right)\right] - 0.4977 \quad \text{(Eq.20)}$$

The B value is given by the slope of the straight line of the plot *B.t* against *t.* More ever, B can be used to calculate the intraparticle diffusion coefficient D*i* using the equation $B= \pi^2 Di/d^2$ where **d** is the radius of the adsorbent particle assumed to be spherical.

The Plotting of *B.t versus t* for both adsorbents are depicted in Figure 4 (the saturation region was not represented). As shown in this figure, the adsorption of MBT demonstrates a linear relationship and has two and one stages when CA and BN are used respectively. The values of the constant B and the regression coefficients are given in Table 4.

In the case of activated carbon, B.t grows with contact time following two different slopes. The first is very fast and is located in the first two minutes, while the second is slower. However, both segments do not pass through the origin, which allows deducing that intraparticle diffusion is not the only important step controlling adsorption kinetics. The two diffusion segments were related to the different diffusion rates attributed to the different pore sizes in terms of macropores, mesopores and micropores and/or to the low quantities in solution phase as previously mentioned in the case of Morris and Weber model.[16]

The Bentonite adsorption towards MBT is characterized by a single line indicating the homogeneity of these sorbent pores. Moreover, the straight line passes very close to zero, which indicates that the retention process is dominated by intraparticle diffusion. Bentonite also presents a Boyd constant 1.83 times higher than that of activated carbon.

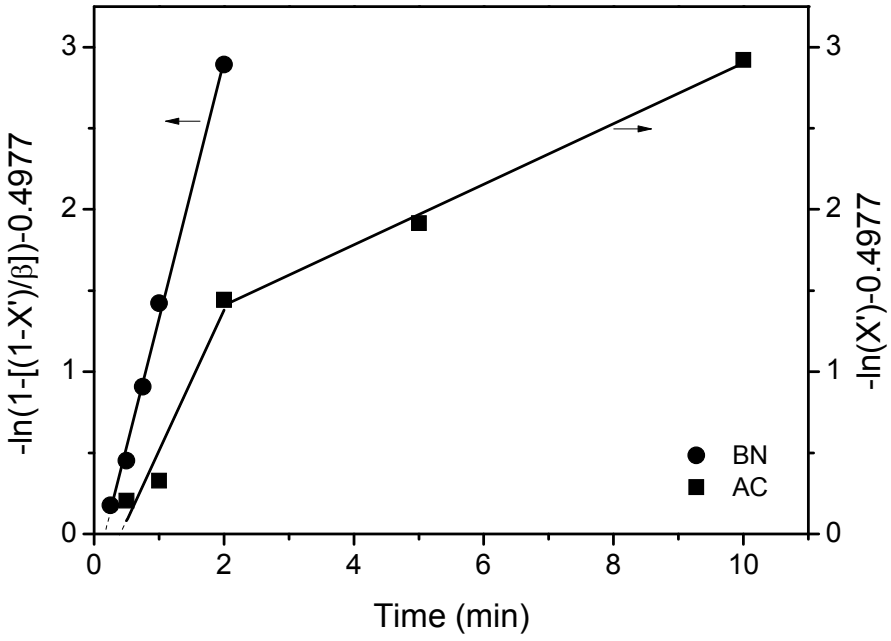

Fig. 4 – Boyd plots for the kinetic modelling of MBT adsorption.

Urano and Tachikawa Model

Furthermore, the Urano and Tachikawa kinetic model, similar to that of Boyd, was also used to determine the actual rate-controlling step involved in the MBT adsorption on both used adsorbents. The Urano and Tachikawa kinetics equation is expressed as:[21,22]

$$-ln\left[1-\left(\frac{q_t}{q_e}\right)^2\right]=\frac{4\pi^2.D_i}{d^2}.t=k_i.t \quad \text{(Eq.21)}$$

with k_i: Intraparticle diffusion rate constant,

D_i : Diffusion coefficient through the solid.

In the case of activated carbon, two stages model, Eq. 22 becomes:

$$-ln[X'.(2-X')]=\frac{4\pi^2.D_i}{d^2}.t=k_i.t \quad \text{(Eq.22)}$$

while with Bentonite, three stages model, the equation describing Urano and Tachikawa model can be modified as:

$$-ln\left[1-\left(\frac{1-X'}{\beta}\right)^2\right]=\frac{4\pi^2.D_i}{d^2}.t=k_i.t \quad \text{(Eq.23)}$$

Changes in the sorption capacity of the two sorbent with time according to this model are shown in Figure 5. As expected, Figure 5 shows that the results are very similar to those obtained with the Boyd model. From the slope and intercept of the obtained straight line, the corresponding constant values for each adsorbent provide the respective kinetic constants k_i and R^2 parameters. The estimated values are reported in Table 4. According to these results, the Urano and Tachikawa model confirms that of Boyd one namely the mono and the multinearity with BN and AC, respectively, as well as the more rapid diffusion of the substrate through the clay compared to carbon. It is worth noting that the straight line describing the diffusion through bentonite passes very close to the original, which demonstrates once more that intraparticle diffusion, *i.e.* the transfer of MBT molecules across the boundary in solution to the interfoliar space layer, is the mechanism that controls the adsorption process.

Elovich Model

One of the most useful models for describing the adsorption kinetics is the Elovich model expressed as:[23-25]

$$\frac{dq_t}{dt}=a.e^{-b.q_t} \quad \text{(Eq.24)}$$

where ***a*** is the adsorption initial rate (at t = 0, dq_t/dt = ***a***) and b is a constant related to the external surface of area. Taking account of the initial conditions, q_t = 0 at t = 0, integration of Eq.24 leads to:

$$q_t=\frac{1}{b}ln(a.b)+\frac{1}{b}ln\left(t+\frac{1}{a.b}\right) \quad \text{(Eq.25)}$$

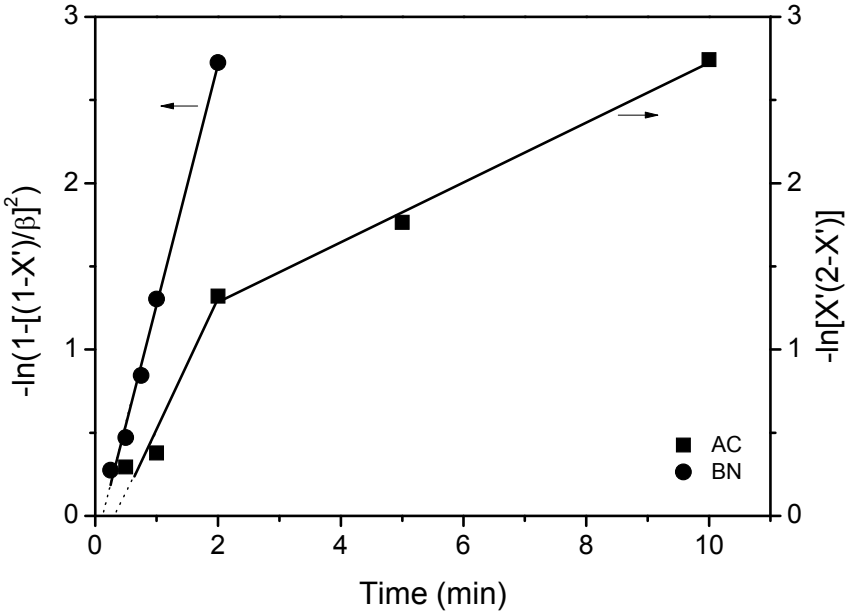

Fig. 5 – Urano and Tachikawa plots for the kinetic modelling of MBT adsorption.

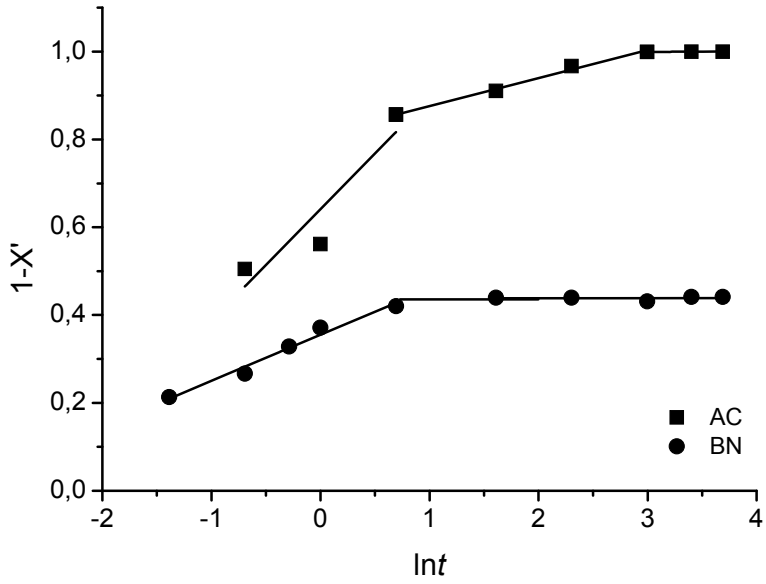

Fig. 6 – Elovich plots for the kinetic modelling of MBT adsorption.

where 1/(a.b) is generally very low compared to the time:

$$q_t = \frac{1}{b} ln(a.b) + \frac{1}{b} ln(t) \quad \text{(Eq.26)}$$

Application of this equation to the two and three stages models allows writing:

$$1 - X^t = \frac{q_2(t)}{q_2(\infty)} = \frac{1}{b'} ln(a.b) + \frac{1}{b'} ln(t) \quad \text{(Eq.27)}$$

where b' = b.$q_2(\infty)$. Eq.27 was used to correlate experimental data by plotting the curves (1-X') against ln (t). As clearly shown in Figure 6, modelling presents multinearity in the case of CA, which demonstrates once more the change in the adsorption kinetics during contact time. Figure 6 also indicates that Elovich equation is not compatible with the experimental data in the first stage (R^2 = 0.7355). With regard to the second step, the perfect curve linearity (R^2 = 0.9867) indicates that this model is well verified and thus confirms the type of chemical reaction of MBT on activated carbon adsorption. The third linear curve, parallel to the ln(t) axis, corresponds to the saturation.

With the clay, the curve corresponding to a single stage is perfectly linear as also shown in Figure 6. The values of the various adsorption kinetic parameters, b', b, a and 1/(ab), for both adsorbents calculated from this kinetic model are given in Table 4.

Avrami Model

To explain more clearly the single linearity with Bentonite and the multinearity with activated carbon, the Avrami model was also used. This model was successfully used to fit the experimental data in adsorption studies of mineral or organic substances on different kinds of adsorbents.[26-28] The adsorption fraction *versus* time is expressed as:

$$\frac{q_t}{q_e} = 1 - e^{-(kt)^n} \quad \text{(Eq.28)}$$

In this equation, k is the Avrami kinetic constant and n is a constant which provides information about the adsorption mechanism changes.

In the case of AC, and after the linearization, the Avrami expression becomes:

ln[-lnX'] = n.lnk + n.lnt (Eq.29)

with Bentonite, we have:

$$\ln\left[-\ln\left(1 - \frac{1}{\beta}(1 - X^t)\right)\right] = n.\ln k + n.\ln t \quad \text{(Eq.30)}$$

The linear plots of Avrami model for both used adsorbents are shown in Figure 7. A comparison of experimental and theoretical values calculated according to this model, for both used adsorbent, is shown in Fig. 7. It illustrates the formation of one and two linearized regions in relation to the contact time for bentonite and AC respectively. In the case of AC, the third region is related to the saturation. The slope and the intercept of each straight line provide the n and k values. Table 4 lists the results, with R^2, indicating the good fitting of the Avrami equation for the adsorption of MBT on AC and Bentonite.

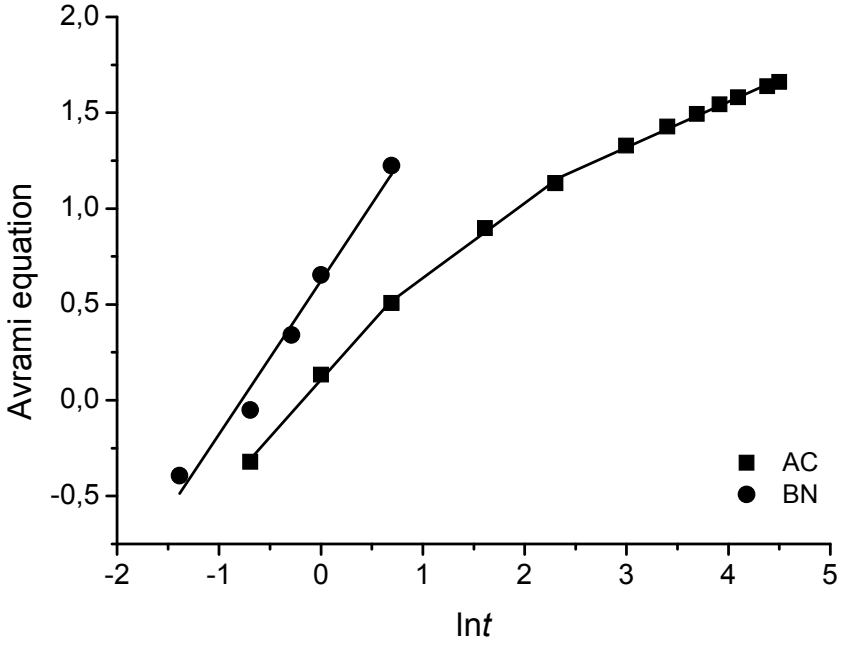

Fig. 7 – Avrami plots for the kinetic modelling of MBT adsorption.

Kinetics order

The order of reaction is a very important parameter in determining the reaction mechanisms. The two orders, one and two, are the most cited in the literature. Kinetics of order one is typically described by the Lagergren equation:[29,30]

$$-\ln\left(1-\frac{q_t}{q_e}\right)=k_1.t \qquad \text{(Eq.31)}$$

where k is the pseudo first order rate constant and q_e the amount adsorbed at equilibrium.

In the case of AC, this relation becomes:

$$-\ln(X')=k_1.t. \qquad \text{(Eq.32)}$$

or $X = \xi_2 . e^{-k1.t}$

Whereas with Bentonite, Lagergren equation can be written as follows:

$$\ln(X-\omega)=\ln(\xi_2-\omega)-k_1.t \qquad \text{(Eq.33)}$$

This is the linear form of:

$$X = (\xi_2 - \omega).e^{-k1.t} + \omega$$

In this study, the application of Eq.33 and E.32 shows that the kinetics is not order one for both adsorbents (Results not shown). This result was expected, given the fact that adsorption of MBT was brought to equilibrium within a short period of time.

However, the kinetics of pseudo-second order is usually represented by Ho equation:[31,32]

$$\frac{t}{q_t}=\frac{1}{k_2.q_e^2}+\frac{1}{q_e}.t \qquad \text{(Eq.34)}$$

This can also be written in the following form:

$$\frac{t}{q_t/q_e}=\frac{1}{k_2.q_e}+t \qquad \text{(Eq.35)}$$

with AC, it can therefore easily deduct another relationship giving X according to time:

$$\frac{t}{1-X'}=\frac{1}{k_2.q_e}+t \qquad \text{(Eq.36)}$$

The comparison of this linear equation with Eq.7 leads to the following conclusions:

i) the parameter α, seen above, is equal to the factor $k_2.q_e$

ii) half-life, corresponding to $X = \xi_2/2$, is the y-intercept or $t_{1/2} = 1/(k_2.q_e) = 1/\alpha$.

Plots of t/(1–X') *versus* t can be represented to verify the pseudo-second-order kinetics. The y-intercept is expected to deduct the value of $k_2.q_e$ and therefore to find α and $t_{1/2}$, but also the calculation of k_2. The slope is equal to unity. As can be seen from Fig.8, the pseudo-second order rate equation is appropriate for the whole adsorption process. In addition, the straight line, with a slope equal to 0.9895, does not pass through the origin. The fitted correlation parameters are summarized in Table 5.

In the case of Bentonite we get:

$$\frac{t}{1-X^t} = \frac{1}{\beta . k_2 . q_e} + \frac{1}{\beta} t = \frac{1}{\beta^2 . k_2 . q_2(\infty)} + \frac{1}{\beta} t \qquad \text{(Eq.37)}$$

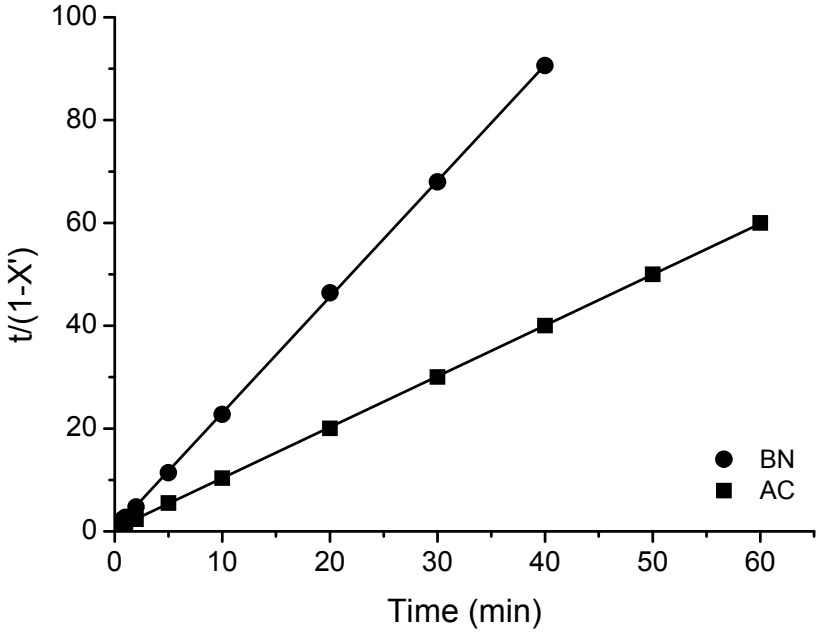

Fig. 8 – Pseudo-second order plots for the kinetic modelling of MBT adsorption.

Table 5

Results of the pseudo-second order kinetic model

	slope	intercept	$k_2.q_e$ (min^{-1})	β_{cal}	$t_{1/2}$ (min)	k_2 ($mg^{-1}.g.\ min^{-1}$)	R^2
CA	0.9895	0.4749	2.106	/	0.475	0.0749	0.9999
BN	2.2562	0.4858	4.644	0.443	/	0.2741	0.9998

For β =1, we find Eq.36 obtained with activated carbon. Regarding the kinetics parameters, we can deduce the calculated value of β and $t_{1/2} = \frac{\beta}{(2\beta-1)} \times \frac{1}{\alpha} = \frac{\alpha}{\beta} - 2\gamma$. Thus, these kinetic parameters can be determined by tracing the straight line t/($1-X^t$) vs *t*. Figure 8 shows the application of this equation to the obtained results and the values of all kinetic parameters are summarized in Table 5. In this case, the half-life, greater than the time required for the equilibrium, was not achieved (β is less than 0.5).

It is worth noting that, for AC and BN, the R^2 values are higher than 0.999, and exceed those obtained with all other models. Thus, the adsorption process follows best the kinetics of pseudo-second order, confirming the chemical sorption of MBT on both studied adsorbents.

EXPERIMENTAL

Materials

2-Mercaptobenzothiazole (MBT, 98%), provided by the Aldrich company, was used as received. An active carbon of vegetable origin and natural bentonite from Magnia, west of Algeria, were used as adsorbents. Bentonite is composed of more than 82% of montmorillonite. Before use, both adsorbents have been dried in an oven at 105 °C for 24 hours and stored in desiccators until use.

Experimental procedure

MBT stock solution was prepared by adding an excess of solid reagent to a volume of deionised water. After 48 hours of agitation, the solution is filtered through a 0.45 µm membrane filter. The concentration of filtered solution is determined by UV-visible spectrometry. This solution was then subsequently diluted to required concentration by deionised water.

Adsorption device

All experiments were conducted in a Pyrex reactor equipped with a double envelope allowing circulation of water.

The dispersion of solid particles, coal or clay, is provided by a magnetic stirrer. In order to control the solution's temperature, the reactor has been linked to a circulator bath. At regular time interval, aliquots, about 4 mL, in triplicate were taken and the adsorbent is separated from the solution by filtration (0.45 μm). Here, only the average values were reported and used in the calculation and only the results obtained in optimal conditions of pH, temperature, agitation speed, MBT initial concentration and adsorbent dose, are presented.

Analysis

The specific surface area, the pore volume and the pore diameter distribution of the two absorbents have been determined, according to BET method, using a device (Surface Area Analyser) BECKMAN Coulter SA310, The particle diameter was also determined for both adsorbents.

The concentration of MBT solution was measured using a spectrophotometer "Helios α-Unicam Sperctronic". It should be noted that calibration graph of absorbance and concentration was preliminary established by plotting known concentrations versus absorbance at a wavelength of 320 nm.

CONCLUSIONS

In this paper, adsorption of MBT on activated carbon and Bentonite was investigated in batch system. Based on the literature data and the fact that the adsorption process was very fast in the early stage, two models were developed to describe the sorption kinetics. Two-stage model was well adapted to the CA, while the three stage model was used with BN. For both adsorbents, linearized equations describing all kinetics of the studied models, namely those of Weber and Morris, Boyd, Urano and Tachikawa, Elovich, Avramiand pseudo-second order kinetic, were expressed by the X parameter, fraction of the residual in solution, versus the contact time. The mass transfer diffusion of MBT molecules follows pore diffusion in both adsorbents. Several kinetic parameters were gathered and/or calculated from the various studied equations. The Application of all equations obtained from the different kinetic models shows that this approach is effective for the study of adsorption kinetics in parallel with the classical method.

Acknowledgments: The authors express their sincere thanks to the Ministry of Higher Education and Scientific Research of Algeria for supporting this work.

REFERENCES

1. K. Y. Foo and B. H. Hameed, *J. Hazard. Mater.*, **2009**, 171, 54.
2. A. Dabrowski, *J. Adv.Colloid. Interf .Sci.,* **2001,** 93, 135.
3. M. D. LeVan, G. Carta and C. M. Yon, In *Perry's Chemical Engineers'Handbook,* 7th ed, McGraw-Hill, New York, 1997, p. 16.
4. J. C. P. Vaghetti, E. C. Lima, B. Royer, N. F. Cardoso, B. Martins and T. Calvete, *J. Sep.Sci. Technol.,* **2009**, 44, 615.
5. A. Kumar, Sh. Kumar and Su. Kumar, *J. Carbon.,* **2003**, 41, 3015.
6. J. P. Chen, S. Wu and K. H. Chong, *J. Carbon.*, **2003**, 41, 1979.
7. S. B. Kim, I. Hwang, D. J. Kim, S. Lee and W.A. Ury, *J. Toxicol. Chem.,* **2003**, 22, 2306.
8. J. W. Choi, N. C. Choi, S. J. Lee and D. J. Kim, *J. Colloid. Interf. Sci.*, **2007**, 314, 367.
9. J. W. Choi, S. G. Chung, D. J. Kim and C. E. Lee, *J. Curr. Appl. Phys.*, **2008**, 8, 559.
10. J. W. Choi, K. S. Yang, D. J. Kim and C. E. Lee, *J. Curr. Appl. Phys*., **2009**, 9, 694.
11. S. J. Lee, S. G. Chung, D. J. Kim, C. E. Lee and J. W. Choi, *J. Curr. Appl. Phys*., **2009**, 9, 1323.
12. H. De Wever, K. De Moor and H. Verachtert, *J. Appl. Microbiol. Biot*., **1994**, 42, 631.
13. O. Fiehn, G. Wegener, J. Jochimsen and M. Jekel, *J. Water Res*., **1998**, 32, 1075.
14. R. S. Juang, F. C. Wu and R. L. Tsing, *J. Colloid Surf. A. Physicochem. Eng. Aspect.*, **2002**, 201, 191.
15. G. F. Malash and M. I. El-Khaiary, *J. Colloid Interf. Sci.*, **2010**, 348, 537.
16. S. J. Allen, G. McKay and K. Y. H. Khader, *J. Environ. Pollut.*, **1989**, 56, 39.
17. D. Kavitha and C. Namasivayam, *J. Chem. Eng.,* **2008**, 139, 453.
18. G. E. Boyd, A. Adamson and L. S. Myers Jr, *J. Am. Chem. Soc*., **1947**, 69, 2836.
19. D. Reichenberg, *J. Am. Chem. Soc.*, **1953**, 75, 589.
20. R. Qadeer, *J. Colloid Surf A.*, **2007**, 293, 217.
21. K. Urano and H. Tachikawa, *J. Ind. Eng. Chem. Res.*, **1991**, 30, 1897.
22. M. Jansson-Charrier, E. Guibal, J. Roussy, B. Delanghe and P. L. Cloirec, *J. Wat. Res.*, **1996**, 30, 465.
23. S. H. Chien and W. R. Clayton, *J. Soil. Sci. Soc. Am*., **1980**, 44, 265.
24. R. L. Tseng, F. C. Wu and R. S. Juang, *J. Carbon.*, **2003, 41**, 487.
25. Z. Reddad, C. Gerente, Y. Sandres and P. L. Cloirec, *J. Environ. Sci. Technol.*, **2002**, 36, 2067.
26. A. R. Cestari, E. F. S. Vieira, J. D. S. Matos and D. S. C. dos Anjos, *J. Colloid Interf. Sci.,* **2005**, 285, 288.
27. D. S. F. Gay, T. H. M. Fernandes, C. V. Amavisca, N. F. Cardoso, E. V. Benvenutti, T. M. H. Costa and E. C. Lima, *Desalination*., **2010**, 258, 128.
28. A. M. M. Vargas, A. L. Cazetta, M. H. Kunita and T. L. Silva, *J. Chem. Eng.*, **2011**, 168, 722.
29. S. Azizian, *J. Colloid Interf. Sci.*, **2004**, 276, 47.
30. V. C. Srivastava, M. M. Swamy, D. Malli, B. Prasad and I. M. Mishra, *J. Colloid. Surf A*., **2006**, 272, 89.
31. Y. S. Ho and G. McKay, *J. Process Biochem.*, **1999**, 34, 451.
32. Y. S. Ho and G. McKay, *J. Wat. Res*., **2000**, 34, 735.